Journal of Seismology (2006) **10:** 213–224
DOI: 10.1007/s10950-005-9009-4

A forward test of the precursory decelerating and accelerating seismicity model for California

B.C. Papazachos, E.M. Scordilis, C.B. Papazachos & G.F. Karakaisis
Geophysical Laboratory, School of Geology, Aristotle University, Thessaloniki 54124, Greece
E-mail: manolis@geo.auth.gr, costas@lemnos.geo.auth.gr, karakais@geo.auth.gr

(Received 7 August 2003; accepted 19 December 2005)

Key words: Accelerating strain, decelerating strain, earthquake prediction, California

Abstract

Accelerating strain energy released by the generation of intermediate magnitude preshocks in a broad (critical) region, and decelerating energy released in a narrower (seismogenic) region, is considered as a distinct premonitory pattern useful in research for intermediate-term earthquake prediction. Accelerating seismicity in the broad region is satisfactorily interpreted by the critical earthquake model and decelerating seismicity in the narrower region is attributed to stress relaxation due to pre-seismic sliding. To facilitate the identification of such patterns an algorithm has been developed on the basis of data concerning accelerating and decelerating preshock sequences of globally distributed already occurred strong mainshocks. This algorithm is applied in the present work to identify regions, which are currently in a state of accelerating seismic deformation and are associated with corresponding narrower regions, which are in a state of decelerating seismic deformation in California. It has been observed that a region which includes known faults in central California is in a state of decelerating seismic strain release, while the surrounding region (south and north California, etc.) is in a state of accelerating seismic strain release. This pattern corresponds to a big probably oncoming mainshock in central California. The epicenter, magnitude and origin time, as well as the corresponding model uncertainties of this probably ensuing big mainshock have been estimated, allowing a forward testing of the model's efficiency for intermediate-term earthquake prediction.

Introduction

Prediction of an individual earthquake is a very difficult and at present unsolved problem. Attempts for short-term prediction (time uncertainty of the order of days to weeks) during the last four decades led to the conclusion that such prediction is not possible given the present level of the relevant scientific knowledge (Wyss, 1997). Long-term earthquake prediction (time uncertainty of the order of decades) is not an easy target either. The physical process of generation of a strong earthquake in a fault is characterized by properties of deterministic chaos. Thus, very accurate knowledge of this process is needed to predict the next strong earthquake (Jaumé and Sykes, 1999) but such knowledge is not feasible at present. It seems, however, that there is more hope for intermediate-term earthquake prediction (uncertainties of the order of a few years) on the basis of precursory seismicity patterns. This can be attributed to predictive properties of such patterns indicated by a wealth of reliable observations and by a physical interpretation provided by the recently developed chaos theory (Evison, 2001). Accelerating generation of intermediate magnitude shocks (preshocks) in a broad (critical) region and decelerating generation (relative quiescence) of shocks (preshocks) in a narrower (seismogenic) region are two of the most distinct such patterns which have been observed before many strong earthquakes. The simultaneous occurrence of the two patterns in different parts of an area has been

called "doughnut pattern" by Mogi (1969). Empirical relations based on properties of these two patterns are applied in the present work in an attempt to estimate the basic parameters of large probably ensuing mainshocks in California.

A large number of seismological observations show that strong mainshocks are preceded by accelerating generation of intermediate magnitude preshocks (Tocher, 1959; Mogi, 1969; Papadopoulos, 1986; Sykes and Jaumé, 1990; Knopoff et al., 1996; Jaumé and Sykes, 1999; Robinson, 2000; Tzanis et al., 2000, among many others). Theoretical work suggests that the process of generation of these preshocks can be considered as a critical phenomenon culminating in a mainshock considered as a critical point (Sornette and Sornette 1990; Allègre and Le Mouel, 1994; Sornette and Sammis, 1995; Rundle et al., 2000). Rock mechanics laboratory experiments also support the idea that rupture in heterogeneous media is a critical phenomenon (Vanneste and Sornette, 1992; Lamaignère et al., 1996; Andersen et al., 1997). Bufe and Varnes (1993) on the basis of a damage mechanics model proposed the following relation for the time variation of the cumulative Benioff strain, S (in Joule$^{1/2}$), released by preshocks at the time, t:

$$S(t) = A + B(t_c - t)^m \tag{1}$$

where t_c is the origin time of the mainshock and A, B, m are parameters determined by the available data. Bowman et al. (1998) suggested the minimization of a curvature parameter, C, chich is defined as the ratio of the root-mean-square error of the power-law fit (relation 1) to the corresponding linear fit error, and used this parameter to identify critical (preshock) regions in various areas since 1950. This approach of identifying and investigating critical regions of previous mainshocks has been further developed and properties of such regions in various seismotectonic regimes (Aegean, Adriatic, Anatolia, Himalaya, Japan, California) have been determined (Papazachos and Papazachos, 2000, 2001; Scordilis et al., 2004; Papazachos et al., 2005a,b).

These properties are expressed by empirical formulas, which relate parameters of a preshock accelerating sequence with the parameters of the following mainshock. For this reason, such empirical formulas have predictive abilities. Papazachos (2001) used relation (1), the minimization of the curvature parameter and such empirical formulas to develop an algorithm, which identifies the critical (circular or elliptical) region of an already occurred strong mainshock. It also identifies currently active critical regions and estimates (predicts) the parameters of probably ensuing mainshocks, which are associated with such critical regions.

The choice of the shape of a critical region is of importance for identifying such regions and several shapes have been used (circular, elliptical, etc). A circular region has the advantage that there is small probability for parts of more than one preshock (critical) regions to be included in such shape. There are, however, very elongated seismic zones for which no solution can be found using circular shapes and reliable such solutions are only found for elliptical shapes. The broad critical region examined in the present work is satisfactorily fitted by both circular and elliptical shapes and the elliptical shape was adopted.

Intermediate-term decrease of seismicity before many strong earthquakes has also been observed. Most of these observations concern decrease of the number (frequency) of mainly small shocks (seismic quiescence) in the fault region of strong earthquakes (Wyss and Habermann, 1988; Scholz, 1988; Wyss, 1997; Chouliaras and Stavrakakis, 2001; Zöller et al., 2002, among others). There are also studies where measures of seismic crustal deformation (Benioff strain, etc.) have been used to show intermediate-term-decrease of preshock seismic activity in the fault region of mainshocks (Kanamori, 1981; Jaumé, 1992; Bufe et al., 1994; Tzanis and Vallianatos, 2003). Physical interpretation of this preshock decrease of seismic activity has been attempted by attributing it to several factors, such as bimodal distribution of fracture strength (Kanamori, 1981), dilatancy hardening (Scholz, 1988) and stress relaxation due to preseismic sliding (Wyss et al., 1981; Kato et al., 1997), with the later being the most probable one.

Papazachos et al. (2004a, b) used data concerning preshocks of strong mainshocks in the Aegean area to show that accelerating seismic strain in the broad critical region is associated with decelerating change of the frequency and magnitude of intermediate magnitude preshocks in the narrower seismogenic region. For this reason time variation of the preshock Benioff strain in the seismogenic region was fitted by a power-law (relation 1) with $m > 1.0$. It has been further shown that the dimension of the seismogenic region, where decelerating seismic deformation occurs, scales with the mainshock magnitude and with the mean long-term strain rate and that the duration of the decelerating

deformation also scales with this rate. Both patterns end at the origin time of the mainshock but their start times differ. The accelerating sequence starts usually earlier, as is explained bellow.

The term "preshocks" used in this study differs from the classical term "foreshocks" because it expresses shocks generated in different space and time scales. Thus, foreshocks are spatially distributed in the "rupture zone" of an oncoming mainshock and the duration of their sequences is relatively small (of the order of days to weeks), while preshocks are distributed in a much broader region and the duration of their sequences is much longer (of the order of years). There are two kinds of preshocks which differ with respect to their spatial distribution: those which are generated in a broad region (critical region) with an accelerating mode (accelerating preshocks) and those which are generated in the "seismogenic region" (the rupture zone and surrounding area) with a decelerating pattern (decelerating preshocks). The linear dimension of a critical region is about eight times larger than the rupture length and about two times larger than the linear dimension of the seismogenic region where decelerating seismic deformation occurs. Decelerating and accelerating preshocks differ also in respect to their time and magnitude distribution, as is shown below.

Seismologists working on earthquake prediction cannot easily test the validity of their results by producing relative data at will (laboratory experiments, etc.). Various methods are used for "retrospective predictions" of already occurred earthquakes (postdictions); however, this approach is not adequate. Forward testing by attempting predictions of future strong earthquakes is necessary for more objective evaluations. In the framework of this strategy, an attempt is made to identify critical regions where accelerating seismic strain currently occurs and which include smaller (seismogenic) regions where decelerating strain occurs in California. The epicentral coordinates, magnitudes and origin times of the corresponding probably ensuing mainshocks have been estimated in order to evaluate the predicting ability of this method by a forward testing procedure.

Model Applied

The model applied in the present work is based on the "accelerating seismic strain" technique, which is a developed form of the time-to-failure technique (Bufe and Varnes, 1993) and on the "decelerating seismic strain" technique, which is a developed form of the seismic quiescence technique (e.g. Wyss and Habermann, 1988; Bufe et al., 1994).

The accelerating seismic strain technique is based on relation (1) as this relation is applied to express the time variation of the accelerating seismic strain ($m < 1.0$) and on the following relations which have been derived (Papazachos et al., 2005a,b) on the basis of global observations concerning preshock (critical) regions of strong ($M = 6.3 - 8.3$) mainshocks:

$$\log R = 0.42M - 0.30 \log s_a + 1.25, \quad \sigma = 0.15 \quad (2)$$

$$\log(t_c - t_{sa}) = 4.60 - 0.57 \log s_a, \quad \sigma = 0.10 \quad (3)$$

$$M = M_{13} + 0.60, \quad \sigma = 0.20 \quad (4)$$

where R (in km) is the radius of the circular preshock (critical) region (or the radius of the equivalent circle in the case of elliptical critical region), s_a (in Joule$^{1/2}$/yr·10^4 km^2) is the rate of the long-term seismic strain per year and per 10^4 km^2 in the critical region, t_{sa} (in yrs) is the start time of the accelerating sequence, t_c is the origin time of the mainshock, M is the magnitude of the mainshock and M_{13} is the mean magnitude of the three largest preshocks.

In order to compare the obtained results regarding the R, M, t_{sa}, values estimated for each mainshock with the relations (2), (3), (4), the probability of each obtained parameter was calculated. For this reason each model parameter was estimated with respect to its expected value, assuming that the deviation of each parameter follows a Gaussian distribution. The average, P_a, of these probabilities is used as a measure of the agreement of the determined parameters with those calculated by these three global relations (Papazachos and Papazachos, 2001). Furthermore, for each point of the investigated area a "quality index", q_a, has been defined (Papazachos et al., 2002) by the formula:

$$q_a = \frac{P_a}{m \cdot C} \quad (5)$$

where C is the curvature parameter, which expresses the degree of deviation from linearity of the time variation of the cumulative Benioff strain (Bowman et al., 1998) and m is the parameter of relation (1) which expresses the degree of acceleration. On the basis of a large sample of data concerning accelerating preshock sequences of mainshocks which occurred in a variety of seismotectonic regimes and had magnitudes between

5.6 and 8.3 (Papazachos and Papazachos, 2000, 2001; Scordilis et al., 2004; Papazachos et al., 2005a,b) the following cut off values have been determined:

$$C \leq 0.60, \quad P_a \geq 0.45, \quad m \leq 0.35, \quad q_a \geq 3.0 \quad (6)$$

Hence, any valid solution in a geographic point of a critical (preshock) region must fulfill these relations. Worldwide observations show that a mean value of m is 0.30, which is in agreement with theoretical considerations (Rundle et al., 1996; Ben-Zion et al., 1999). For these reasons, this value was adopted throughout the present work. The geographic point, Q, for which relations (6) are fulfilled and where the quality index q_a has its largest value is considered as the geometrical center of the critical region. The magnitude, $M_{\min}$, of the smallest preshock of an accelerating preshock sequence for which relations (6) hold and q_a has its largest value is given by the relation:

$$M_{\min} = 0.46M + 1.91 \quad (7)$$

where M is the magnitude of the mainshock (Papazachos, 2003; Papazachos et al., 2005a). Thus, for mainshock magnitudes 6.0, 7.0 and 8.0 the corresponding minimum magnitudes of accelerating preshock sequences are 4.7, 5.1 and 5.6, respectively.

Decelerating seismic strain (Benioff strain) released by intermediate magnitude preshocks in the seismogenic region follows a power-law (relation 1 with $m > 1$) and the relations:

$$\log a = 0.23M - 0.14 \log s_d + 1.40, \quad \sigma = 0.15 \quad (8)$$

$$\log (t_c - t_{sd}) = 2.95 - 0.31 \log s_d, \quad \sigma = 0.12 \quad (9)$$

where α (in km) is the large axis of the elliptical seismogenic region, M is the magnitude of the mainshock, t_{sd} (in yrs) is the start time of the decelerating preshock sequence, and s_d (in Joule$^{1/2}$/yr·10^4 km^2) is the long-term seismic strain rate (long-term seismicity) of the seismogenic region (Papazachos et al., 2005b). A quality index, q_d, can be also defined by the relation:

$$q_d = \frac{P_d \cdot m}{C} \quad (10)$$

where P_d is defined for decelerating seismicity on the basis of the quantities a, M, t_{sd} and the relations (8, 9) as P_a has been defined on the basis of quantities R, M, t_{sa} and relations (2, 3, 4). The following cut-off values have been calculated by the use of data for decelerating preshock sequences of corresponding strong mainshocks occurred in a variety of seismotectonic regimes (Papazachos et al., 2005b):

$$C \leq 0.60, \quad 2.5 \leq m \leq 3.5, \quad P_d \geq 0.45, \quad q_d \geq 3.0 \quad (11)$$

From relations (3) and (9) it can be deduced that the duration of accelerating and decelerating sequences are equal for strain rate $\log s_a = \log s_d = 6.35$. Since for most areas the strain rate is smaller, the accelerating sequence starts usually earlier than the corresponding decelerating sequence. Thus for California (where $\log s \approx 5.0$) the durations of accelerating and of decelerating preshock sequences are about 56 years and 25 years, respectively.

By the use of global data it has been shown (Papazachos et al., 2005b) that the minimum magnitude, $M_{\min}$, of decelerating preshocks for which the best solution (smallest C value) is obtained, is given by the relation:

$$M_{\min} = 0.29M + 2.35 \quad (12)$$

where M is the magnitude of the mainshock. Thus, for mainshock magnitudes 6.0, 7.0 and 8.0 the corresponding values of $M_{\min}$ are 4.1, 4.4 and 4.7, respectively, which are much smaller than the corresponding minimum values (4.7, 5.1 and 5.6) for accelerating preshocks. It is of interest to note that decelerating seismicity which precedes strong mainshocks ($M \geq 6.0$) is also pronounced for intermediate magnitude ($M \geq 4.0$) preshocks. Data for such shocks are easily available.

The Data

Two samples of data are required for the present work: a) the sample of shocks (preshocks) needed to calculate the Benioff strain and its time variation which is fitted by relation (1) and, b) the sample of shocks to calculate the long-term strain rates (s_a, s_d) needed in relations (2, 3, 8, 9). Care has been taken to ensure that the data samples are accurate, homogeneous, large enough and complete. Instrumental data for earthquakes in California have such properties because a dense seismological network is in operation in this area for a relatively long time.

The basic sources of data for earthquakes generated during the last four decades (since 1965) are the bulletins (ISC, 2005; NEIC, 2005; Harvard, 2005), which publish information from global and regional networks. The accuracy of these data (epicenter locations, magnitude values) for intermediate magnitude shocks of this period (1965–2005) is satisfactory for the purposes of the present work, due to the dense network of seismic stations in California. The data of this period, however, are not enough for calculating the long term strain rates (s_a, s_d) and for this reason information from other catalogues and bulletins (i.e. ANSS Composite Earthquake Catalog, etc.) have been also used to expand the data to the past. In order to keep the data accuracy at a similar level we considered only data of stronger shocks for this earlier instrumental period (before 1965). Strain rates were calculated by using data concerning earthquakes with moment magnitudes $M \geq 5.2$ since 1930.

Magnitudes are given in the catalogues in several scales (M_s, m_b, M_L, M_w). All these magnitudes were transformed into the moment magnitude scale, $M_w(=M)$, by appropriate formulas (Scordilis, 2006). Hence, all data used in the present study are homogeneous with respect to magnitude, since all these magnitudes are moment magnitudes or equivalent to moment magnitudes, M.

The sizes of both categories of data samples used in the present study depend on the dimensions of the region considered (critical, seismogenic) which increase with increasing mainshock magnitude (see relations 2, 8). Experience on critical regions of already occurred mainshocks (Papazachos and Papazachos 2000, 2001) suggests that a sample of at least 20 shocks is necessary for reliable results.

The samples of both categories of data used in the present study are complete, that is, include all shocks which occurred in the region during a certain time period and have magnitudes larger than a certain value. Accurate knowledge of this minimum magnitude value is necessary for a reliable estimation of the cumulative Benioff strain and of the long-term strain rate. For this reason the completeness of the data was checked using both the frequency-magnitude and cumulative frequency-magnitude relation. The determined completeness of the catalogue used in the present study is $M \geq 5.2$ since 1930 and $M \geq 4.0$ since 1965 (Karakaisis et al., 2006).

Figure 1 shows a map of California and surrounding area where epicenters of three samples of data are plotted ($M \geq 7.3$ since 1850, $6.8 \leq M \leq 7.2$ since 1900, $5.2 \leq M \leq 6.7$ since 1930). Three sizes of circles are used to show the corresponding magnitude intervals. The year of occurrence and the magnitude of the largest known earthquakes ($M \geq 7.3$) are also shown.

Procedure Followed

The algorithm to identify a critical and the corresponding seismogenic region in order to estimate the magnitude, M, the origin time, t_c, and the geographic coordinates of the epicenter, E, of a probably oncoming mainshock includes three main steps:

a) Identification of the critical (preshock) region is attempted and, if such region exists, estimation of the parameters related to this critical phenomenon, including the mainshock magnitude, M, is performed. For this purpose the broader area (32°N–42°N, 115°W–125°W) of California was separated in a grid of geographic points with a high density (0.2°). Each point of the grid was considered as the center of the circular (or elliptical) critical region and magnitudes of shocks (preshocks) with epicenters in this region were used to calculate parameters of relation (1) and the curvature parameter. Calculation for each point was repeated for a large set of values (~500 sets) of the radius, R, of the region (in cases of elliptical shapes, for several lengths and azimuths, z, of the large axis and for several values of ellipticity, e), of the start time, t_{sa}, of the seismic (preshock) sequence (the end time of the sequence is the 31 October 2005), of the magnitude, M, of the mainshock and of the number of shocks (preshocks), n, with minimum magnitude, $M_{\min}$, defined by relation (7). All valid solutions (which fulfill relations 6) were considered and the geographic point, Q, with the largest value of the quality index, q_a, was taken as the geometric center of the critical region, while the solution (q_a, C, M, R, t_c, $M_{\min}$, n, log s_a, ...) which corresponds to this maximum q_a value was considered as the best solution. Thus, in this step, a value for the magnitude, M, of the probably oncoming mainshock (relations 2, 4) and a value for its origin time, t_c, (relation 3) were estimated.

b) Identification of the regions where decelerating deformation occurs was performed by a similar grid search and optimization approach and the center of each of these regions was defined. All points of the grid are tested as possible centers of the seismogenic region by relations (11). The geographic point which satisfies these relations and corresponds to the largest quality index, q_d, given by relation (10) is considered as the geometric center, F, of the elliptical region where decelerating seismic deformation occurs. During this step a second value for the magnitude of the mainshock is

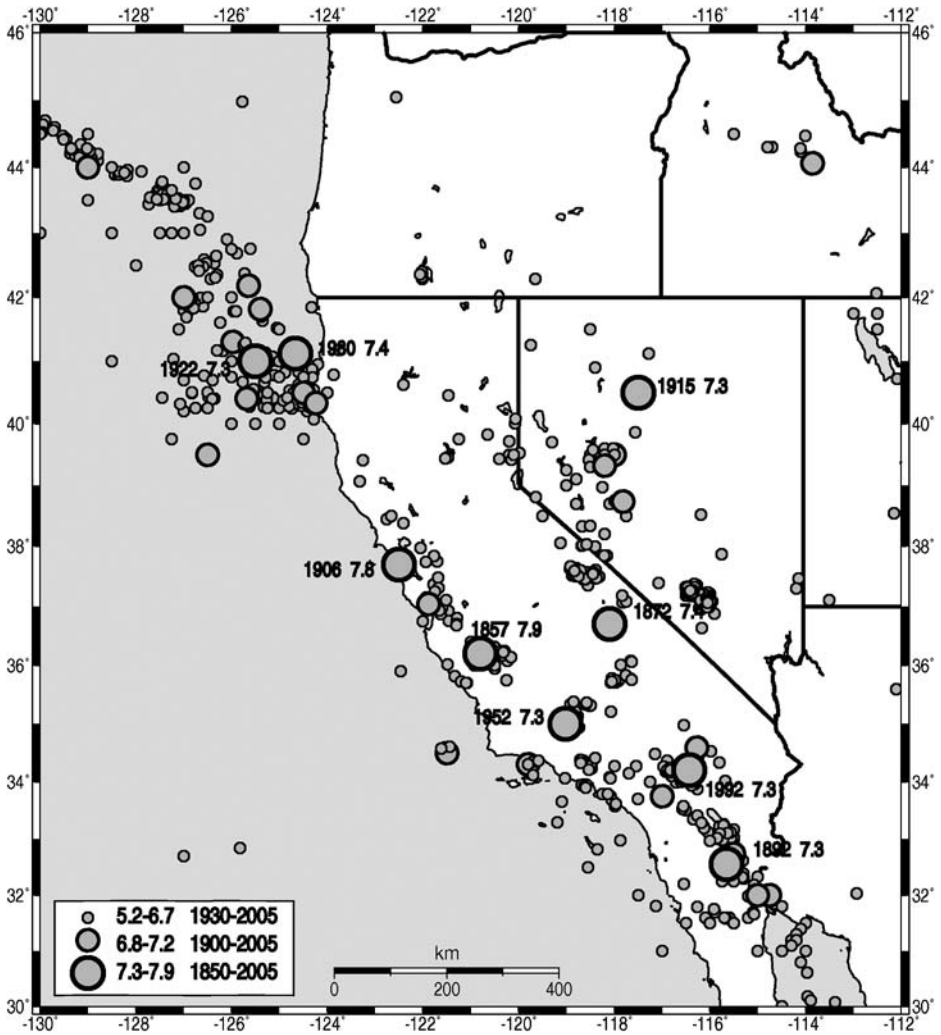

Figure 1. Epicenters of earthquakes in California and surrounding area for three samples of data ($M \geq 7.3$ since 1850, $6.8 \leq M \leq 7.2$ since 1900, $5.2 \leq M \leq 6.7$ since 1930). The year and magnitude for the first sample of large earthquakes are also shown.

calculated (relation 8) and a second value for its origin time (relation 9).

Thus, the average, M, of the two values of magnitude calculated in the first two steps is considered as the magnitude of the probably oncoming mainshock and the average, t_c, of the corresponding two values of origin time is considered as the origin time of the probably oncoming mainshock. Application of this procedure for a retrospective prediction of already occurred globally distributed mainshocks indicates a model uncertainty of ± 0.4 ($=2\sigma$) for the mainshock magnitude and ± 2.5 years for its origin time (Papazachos et al., 2005b).

c) The epicenter location of an oncoming mainshock is mainly based on the location of the region of the decelerating preshocks (seismogenic region) but the location of the region of the accelerating preshocks (critical region) can also contribute to this purpose. Both regions are known before the generation of the mainshock. There are two known geographic points for the seismogenic region, its geometrical center, F, and the center, P_f, of the epicenters of the decelerating preshocks which is considered as the physical center of this region. There are also two known points for the critical region, its geometrical center, Q, and its physical center, P_q, which is the center of the epicenters of the accelerating preshocks.

Papazachos et al. (2005b) used the middle point, D, of the line segment $F P_f$ and the middle point, A, of the

Table 1. Parameters of the elliptical region of accelerating seismic strain (first line) and of the elliptical region of decelerating seismic strain (second line). ϕ, λ, are the geographic coordinates of the geometrical center of the region, M is the estimated mainshock magnitude, t_c is the estimated origin time (in years) for the expected mainshock, m is the parameter of relation (1), C is the curvature parameter, q is the quality index, a (in km) is the length of the large axis of the elliptical region, z is the azimuth (in degrees) of this axis, e is the ellipticity of the region, s (in Joule$^{1/2}$/yr·10^4 km^2) is the mean long-term seismic strain rate in each region, $M_{\min}$ and $M_{\max}$ are the magnitudes of the smallest and largest shock (preshock), n is the number of these shocks, t_s is the start year of the corresponding seismic sequence

Region	ϕ(N), λ(W)	M	t_c	m	C	q	a	z	e	log s	$M_{\min}$	$M_{\max}$	n	t_s
1. California	33.4, 120.0	7.7	2006.9	0.3	0.58	4.7	898	310	0.70	5.03	5.5	7.3	96	1953
2. Centr. California	37.3, 122.1	7.9	2008.3	3.0	0.24	10.4	427	300	0.70	4.94	4.6	6.9	361	1982

line segment QP_q to retrospectively define the epicenter, E, of each of a large number of globally distributed mainshocks with magnitudes between 6.0 and 8.3. It was observed that DE =100km ±40 km and AE = 180±80 km. Based on these results they suggested the following procedure for location of the epicenter of an ensuing mainshock: In the cases where the two circles (D, 100 km; A, 180 km) do not intersect the point of the circle (D, 100 km) which is closer to the circle (A, 180 km) is considered as the predicted mainshock epicenter, E. In the other cases, when the two circles intersect, a unique solution cannot be defined by the previous procedure and D (defined from the decelerating pattern) is considered as the mainshock epicenter. Application of this procedure on already occurred preshock sequences indicates an uncertainty up to 150 km in the epicenter location (Papazachos et al., 2005b).

Results

For California and surrounding area (32°N−42°N, 115°W−125°W) a grid of geographic points was considered and the procedure already described has been applied to identify currently active seismogenic regions, where decelerating seismic strain occurs ($q_d \geq$ 3.0), and critical regions, where accelerating seismic strain occurs ($q_a \geq$ 3.0), for mainshock magnitudes ranging between 6.5–8.0. The results of this procedure are shown in Table 1. In the first line of this table the parameters coming from the accelerating seismic sequence are given (predicted magnitude, M, and origin time, t_c, of the expected mainshock and parameters $m, C, \ldots$ of the accelerating sequences). In the second line of this table, the parameters coming from the decelerating seismic sequence are given.

Table 1 shows that the study of accelerating sequence results in a value of $M = 7.7$ for the magnitude and $t_c = 2006.9$ for the origin time of the mainshock and that the corresponding values from the study of decelerating sequence gives $M = 7.9$ and $t_c = 2008.3$. Therefore, their corresponding average values $M = 7.8$ and $t_c = 2007.6$ can be adopted as the predicted magnitude and origin time of the probably ensuing mainshock.

Figure 2 shows the broad (critical) elliptical region and the narrower (seismogenic) elliptical region in California. Open circles and dots in the figure show epicenters of accelerating and decelerating shocks (preshocks), respectively. In the lower part of the this figure the time variation of the cumulative strain, $S(t)$, in the critical region (accelerating strain, left) and in the seismogenic region (decelerating strain, right) are also shown.

Figure 3a shows the geographical distribution of the quality index, q_d, for the decelerating strain, Figure 3b shows this distribution of the quality index, q_a, for the accelerating strain and Figure 3c the geographical distribution of their difference, $q_d - q_a$. In these figures we also present the geometrical center, F (37.3°N, 122.1°W), the physical center, P_f (37.2°N, 120.0°W), of the seismogenic region where decelerating seismicity occurs, as well as the geometrical center, Q (33.4°N, 120.0°W), and the physical center, P_q (35.6°N, 118.4°W), of the critical region where accelerating strain occurs. This figure shows clearly that decelerating seismic deformation occurs in central California and accelerating seismic deformation occurs in the surrounding area (south California, north California, etc.). Taking these observations under consideration and observations on preshock sequences of already occurred mainshocks which show that q_d takes its largest values close to the mainshock epicenter and that q_a takes its largest values away from this epicenter (Papazachos et al., 2005a,b), we may conclude that central California is

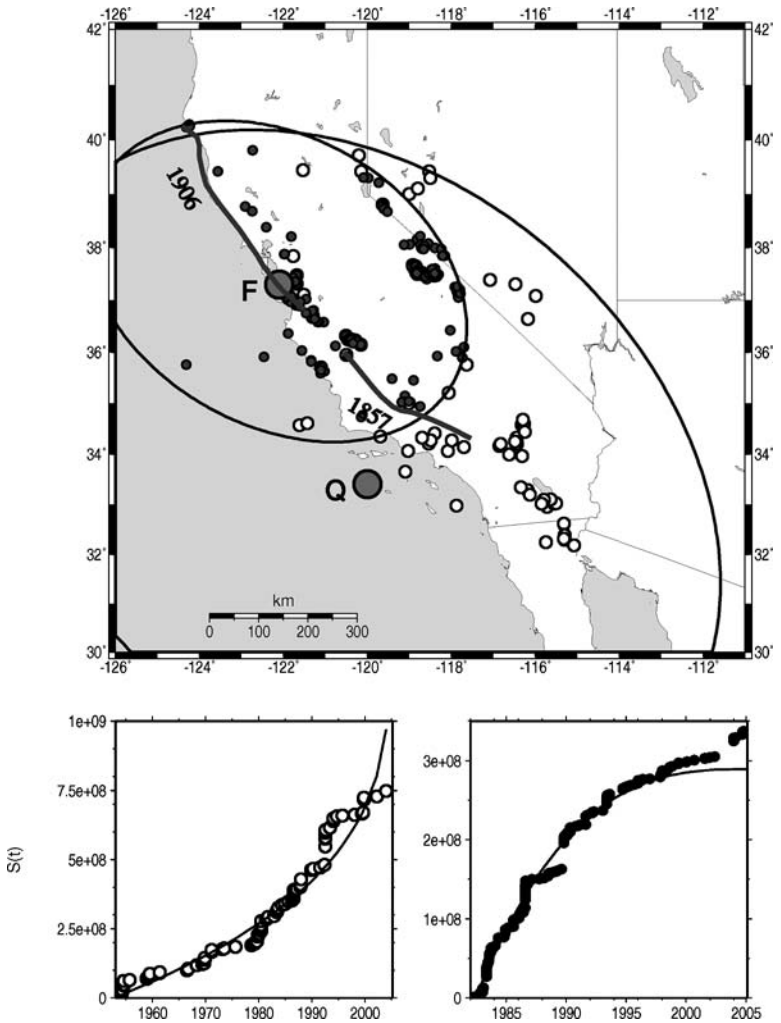

Figure 2. The critical region (large ellipse) where accelerating seismic strain corresponding to a big probably ensuing mainshock and the smaller region (small ellipse) where decelerating seismic strain currently occur in California. Epicenters of accelerating and decelerating shocks (preshocks) are shown by small open circles and dots, respectively. Fault traces of the 1906 ($M = 7.8$) and 1857 ($M = 7.9$) great earthquakes are also shown. Corresponding time variations of accelerating and decelerating strain release are shown in the lower part of the figure.

a candidate region for a probably ensuing mainshock with a big magnitude (∼7.8) during the next five years or so.

The predicted epicenter of this probably ensuing mainshock has been located by the method already described and the use of the geographic coordinates of the centers of the seismogenic region (F, P_f) and of the critical region (Q, P_q). Therefore, this predicted epicenter is E (36.4°N, 120.5°W).

As uncertainties of the parameters of the probably oncoming mainshock we have considered the model uncertainties determined by a retrospective procedure of already occurred mainshocks. Thus, the predicted magnitude and origin time are $M = 7.8 \pm 0.4$ and $t_c = 2007.6 \pm 2.5$ and the predicted epicenter can be located within a circle with center (36.4°N, 120.5°W) and radius up to 150 km. These uncertainties correspond to a probability confidence of ∼75% due to uncertainties in the data and false alarms indicated by tests on synthetic catalogues (Papazachos et al., 2002, 2004a). The probability, P_r, for random occurrence in this circle of such earthquake in the period of 10 years has been also estimated and is less than 10%. This probability was calculated by applying the Gutenberg-Richter recurrence law in the complete sample of data available for California (see Figure 1) and assuming a standard Poisson distribution for the time variation of earthquakes.

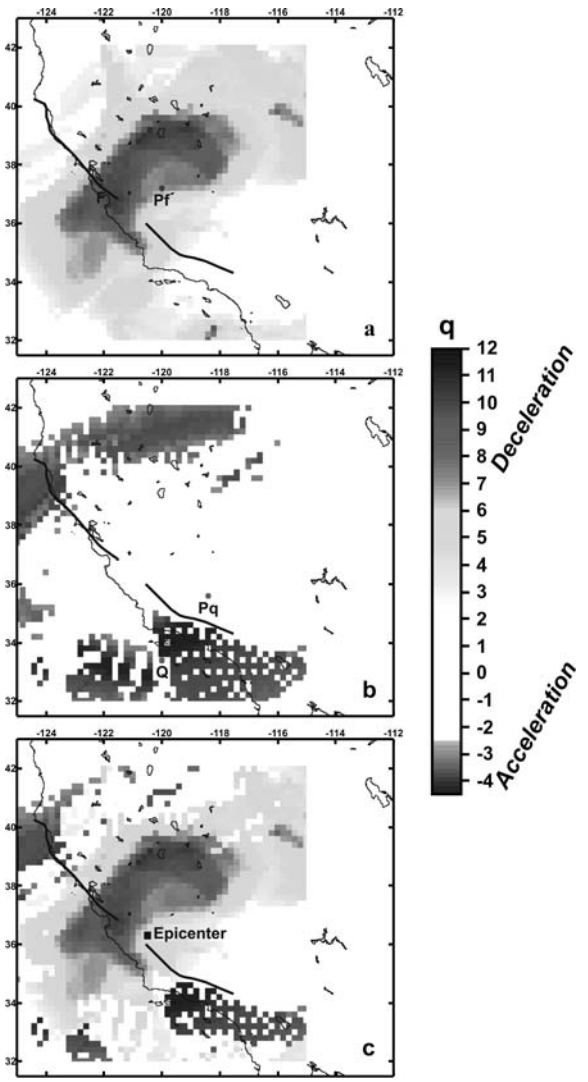

Figure 3. Geographical distribution of the index, q_d, of decelerating seismic strain (a), of the index, q_a, of accelerating seismic strain (b), and of their difference (c). The geographical centers (F, Q) and the physical centers (P_f, P_q) of the seismogenic and critical region, respectively, are also shown. Fault traces of the 1906 ($M = 7.8$) and 1857 ($M = 7.9$) great earthquakes are also shown. The solid square shows the epicenter of the probably ensuing great shock ($M = 7.8 \pm 0.4$).

It is of interest to note that the predicted epicenter (36.4°N, 120.5°W) of this probably oncoming big ($M = 7.8$) earthquake is very close to the epicenter of the Fort Tejon earthquake (9.1.1857, 36.2°N, 120.8°W, $M = 7.9$). This indicates that the southern part of the San Andreas fault will be probably activated during the next five years or so.

Discussion

It has been suggested that the earth's crust is in a state of self-organized criticality (Bak and Tang, 1989). If this occurs in all space and time scales, then earthquakes are inherently unpredictable phenomena. However, it has been recently shown that there are parts of the crust which are not in a state of self-organized criticality (Grasso and Sornette, 1998). On the other hand geological and seismological observations show that characteristic earthquakes in a fault show quasi-periodic behavior and do not follow any power-law distribution. This is supported by proposed inhomogeneous cellular automata which better resemble nature (Sammis and Smith, 1999; Weatherley et al., 2000), by studies of avalanches in physical sand piles (Rosendahl et al., 1994) and by other theoretical work (Ben-Zion et al., 1999). In other words, this information indicates that the generation of a mainshock destroys the self-organized criticality and returns the system to a state far from failure. A period of quiescence follows, after which the process is repeated by rebuilding correlation lengths toward criticality and the next mainshock.

The present work is based on this model of recurrent criticality. This model is also supported strongly by the fact that all studied by us complete samples of globally distributed strong shallow mainshocks were preceded by decelerating in – accelerating out seismic sequences with predictive properties (Papazachos et al., 2005b).

The results of the present work are based on the model which is expressed by empirical relations derived by data of preshock sequences of already occurred mainshocks (Papazachos et al., 2005b). However, most of these relations and relative parameters have been also derived theoretically.

Thus, the basic relation (1) which expresses the time variation of the precursory Benioff strain has been derived on the basis of damage mechanics theory (Bufe and Varnes, 1993) and by principles of the critical point dynamics (Sornette and Sornette, 1990; Sornette and Sammis, 1995). Also, observations on seismic quiescence (decelerating seismicity) have been interpreted by theoretical models such as dilatancy hardening (Scholz, 1988) and stress relaxation due to preseismic sliding (Wyss et al., 1981; Kato et al., 1997). Furthermore, observations show that the exponent, m, of relation (1) has a value equal to 0.3 for accelerating precursory seismicity (Zöller and Hainzl, 2002; Papazachos et al., 2005a) which is in agreement with theoretical considerations and laboratory results which suggest values between 0.25 and 0.33 (Ben-Zion et al.,

1999; Guarino et al., 1999; Rundle et al., 2000; Ben-Zion and Lyakhovsky, 2002). Relation (2) and its scaling coefficients (0.42, −0.30) which have been derived by seismological observations (Papazachos et al., 2005a, b) are in excellent agreement with a relation and its parameters (0.43, −0.33) derived theoretically by Dobrovolsky et al. (1979).

Figure 2 (bottom, left) shows that the strain rate exhibits a declination from its accelerating pattern at the end of the sequence, after the generation of a large earthquake in the beginning of 1990s in southern California (Landers earthquake 28.6.1992, $M = 7.3$). Such declination of the accelerating strain rate in the critical region is often observed during the last years of the critical period. For instance, the largest accelerating preshock of the big San Francisco earthquake (18.4.1906, $M = 7.8$) occurred in southern California (24.2.1892, $M = 7.3$) fourteen years before this big mainshock. To further examine this problem we have studied the time variation of the quality index, q_a, for each of the 46 accelerating preshock sequences investigated by Papazachos et al. (2005b). We have observed that this index increases with time and takes its largest value a few years before the mainshock and then decreases up to the time of the mainshock. It indicates that this declination is a common property of the accelerating preshock sequences.

The pattern identified in the present work dominates the whole California (see Fig. 3) and makes practically almost impossible the search for identification of other such patterns corresponding to smaller mainshocks in this area. We are currently investigating the space, time and magnitude distributions of associated strong shocks (preshocks, postshocks) with respect to their mainshock and expect to be soon able to perform estimation for the strong shocks by which a mainshock is accompanied. Thus, the results of the present work can be of practical importance because identification of regions, which are for several years in seismic excitation (accelerating seismicity) or in seismic quiescence (decelerating seismicity) and the estimation of associated strong shocks can contribute to time dependent seismic hazard assessment.

The present work can be also useful for improving methods on short-term earthquake prediction, since many strong earthquakes are preceded by foreshocks which occur shortly before the mainshock and their foci are close to its focus. Several properties of foreshocks, such as time variation of their frequency according to a power law and magnitude distribution with relative small "b value" have been suggested for short-term earthquake prediction. However, foreshocks are usually of small magnitude and their number is often limited, rendering them indistinguishable from the background seismicity. In other words, seismologists do not know where and when to look for foreshocks. The results of the present work indicate that looking in a seismic zone during a critical period, when seismic quiescence (decelerating strain) is observed in this zone and seismic excitation occurs in a broader region can possibly facilitate the observation of foreshocks in this zone near the end of the critical period (see relations 3, 9). A shorter seismic excitation after an intermediate-term seismic quiescence in a fault zone is supported both by observations (Papazachos et al., 2004b), as well by simulation models (Hainzl, et al., 2000). Figure 2 (bottom, right) shows such an increase of seismic activity at the last part of the decelerating sequence, which probably indicates that the origin time of the mainshock is approached.

It is generally accepted that the road to prediction of individual earthquakes for social purposes is a hard and probably long process. At present we are at a stage of searching if such a road could be found. The present work should be considered as belonging in this frame of efforts. It must be emphasized, however, that forward testing must be attempted for many future mainshocks. We have already made such attempts for the whole Mediterranean and surrounding area (Papazachos et al., 2005c) and we are also currently working for different regions.

Acknowledgments

We are grateful to the Editor and the three anonymous reviewers whose comments and valuable suggestions helped to improve the quality of the manuscript. We also would like to thank Wessel & Smith (1995) for freely distributing the GMT software that was used to produce most of the figures of the present study. This work has been partly financed by the Greek Earthquake Planning & Protection Organization (OASP) under project 20242 Aristotle Univ. Thessaloniki Research Committee and is a Geophysical Lab. Univ. Thessaloniki contribution #630/2003.

References

Allègre, C.J. and Le Mouel, J.L., 1994, Introduction of scaling techniques in brittle failure of rocks, *Phys. Earth Planet. Inter.* **87**, 85–93.

Andersen, J.V., Sornette, D. and Leung, K.T., 1997, Tri-critical behavior in rupture induced by disorder, *Phys. Rev. Lett.* **78**, 2140–2143.

ANSS *Composite earthquake Catalogue*, 2005, http://www.ncedc.org/anss/.

Bak, P. and Tang, C., 1989, Earthquakes as self organized critical phenomenon, *J. Geophys., Res.* **94**, 15535–15637.

Ben-Zion, Y., Dahmen, K., Lyakhovsky, V., Ertas, D. and Agnon, A., 1999, Self-driven mode switching of earthquake activity on a fault system, *Earth. Planet. Sci. Lett.* **172**, 11–21.

Ben-Zion, Y., and Lyakhovsky, V., 2002, Accelerating seismic release and related aspects of seismicity patterns on earthquake faults, *Pure and Appl. Geoph.* **159**, 2385–2412.

Bowman, D.D., Quillon, G., Sammis, C.G., Sornette, A. and Sornette, D., 1998, An observational test of the critical earthquake concept, *J. Geophys. Res.* **103**, 24 359–24372.

Bufe, C.G. and Varnes, D.J., 1993, Predictive modeling of seismic cycle of the Great San Francisco Bay Region, *J. Geophys. Res.* **98**, 9871–9883.

Bufe, C.G., Nishenko, S.P. and Varnes, D.J., 1994, Seismicity trends and potential for large earthquakes in Alaska-Aleutian region, *Pure Appl. Geophys.* **142**, 83–99.

Chouliaras, G. and Stavrakakis, G., 2001, Current seismic quiescence in Greece: Implications for seismic hazard, *J. Seismology*, **5**, 595–608.

Dobrovolsky, J.P., Zubkov, S.I. and Miachkin, B.J., 1979, Estimation of the size of earthquake preparation zones, *Pure Appl. Geophys.* **117**, 1025–1044.

Evison, F.F., 2001, Long-range synoptic earthquake forecasting: an aim for the millennium, *Tectonophysics*. **333**, 207–215.

Grasso, J.R. and Sornette, D., 1998, Testing self organized criticality by induced seismicity, *J. Geophys. Res.* **103**, 29965–29998.

Guarino, A.S., Ciliberto, S. and Garcimartin, A., 1999, Failure time and microcrack nucleation, *Europhys. Lett.* **47**, 456–461.

Hainzl, S., Zoller, G., Kurths, J. and Zschau, J., 2000, Seismic quiescence as an indicator for large earthquakes in a system of self-organized criticality, *Geophys. Res. Letters*. **27**, 597–600.

Harvard Seismology (HRVD), 2005, *CMT catalogue*, http://www.seismology.harvard. edu/CMTsearch.html.

International Seismological Centre (ISC), 2005. On-line Bulletin, Internat. Seis. Cent., Thatcham, United Kingdom, http://www.isc.ac.uk/Bull.

Jaumé, S.C., 1992, Moment release rate variations during the seismic circle in the Alaska-Aleutians subduction zone, extended abstract, *Proceed. Wadati Conference on Great Subduction Earthquakes, University of Alaska,* 123–128.

Jaumé, S.C. and Sykes, L.R., 1999, Evolving towards a critical point: a review of accelerating seismic moment/energy release rate prior to large and great earthquakes, *Pure Appl. Geophys.* **155**, 279–306.

Kanamori, H., 1981, The nature of seismicity patterns before large earthquakes. In *Earthquake Prediction, an International Review, M. Ewing, Series 4, Simpson, D. and Richards, P., editors, Am. Geophys. Union, Washington, D.C.,* 1–19.

Karakaisis, G.F., Scordilis, E.M., Papazachos, C.B. and Papazachos, B.C., 2006, A catalogue of earthquakes in California for the period 1901–2005. Publ. Geoph. Laboratory, University of Thessaloniki.

Kato, N., Ohtake, M. and Hirasawa, T., 1997, Possible mechanism of precursory seismic quiescence: Regional stress relaxation due to preseismic sliding, *Pure Appl. Geophys.* **150**, 249–267.

Knopoff, L., Levshina, T., Keillis-Borok, V.J. and Mattoni, C., 1996, Increased long-range intermediate-magnitude earthquake activity prior to strong earthquakes in California, *J. Geophys. Res.* **101**, 5779–5796.

Lamaignère, L., Carmona, F. and Sornette, D., 1996, Experimental realization of critical thermal fuse rupture, *Phys. Res. Lett.* **77**, 2738–2741.

Mogi, K., 1969, Some features of the recent seismic activity in and near Japan II. Activity before and after great earthquakes, *Bull. Earthquake Res. Inst.*, Univ. Tokyo **47**, 395–417.

National Earthquake Information Center (NEIC), 2005, *On-line Bulletin, USGS/NEIC (PDE) 1973 – Present,* http://neic.usgs.gov/ .

Papadopoulos, G.A., 1986, Long term earthquake prediction in western Hellenic arc, *Earthquake Pred. Res* **4**, 131–137.

Papazachos, B.C. and Papazachos, C.B., 2000, Accelerated preshock deformation of broad regions in the Aegean area, *Pure Appl. Geophys.* **157**, 1663–1681.

Papazachos, B.C., Karakaisis, G.F., Papazachos, C.B. and Scordilis, E.M., 2005c, Perspectives for earthquake prediction in the Mediterranean and contribution of geological observations, *J. Geol. Soc.*, (in press).

Papazachos, C.B., 2001, An algorithm of intermediate-term earthquake prediction using a model of accelerating seismic deformation, *2nd Hellenic Conference on Earthquake Engineering and Engineering Seismology, 28–30 November 2001*, 107–115.

Papazachos, C.B., 2003, Minimum preshock magnitude in critical regions of accelerating seismic crustal deformation, *Boll. Geof. Teor. Applic.* **44**, 103–113.

Papazachos, C.B. and Papazachos, B.C., 2001, Precursory accelerating Benioff strain in the Aegean area, *Ann. Geofis.* **144**, 461–474.

Papazachos, C.B., Karakaisis, G.F., Savvaidis, A.S. and Papazachos, B.C., 2002, Accelerating seismic crustal deformation in the southern Aegean area, *Bull. Seism. Soc. Am.* **92**, 570–580.

Papazachos, C.B., Karakaisis, G.F., Scordilis, E.M. and Papazachos, B.C., 2004a, Probabilities of activation of seismic faults in critical regions of the Aegean area, *Geophys. J. Int.* **159**, 679–687.

Papazachos, C.B., Scordilis, E.M., Karakaisis, G.F. and Papazachos, B.C., 2004b, Decelerating preshock seismic deformation in fault regions during critical periods, *Bull. Geol. Soc. Greece* **36**, 1–9.

Papazachos, C.B., Karakaisis, G.F., Scordilis, E.M. and Papazachos, B.C., 2005a, Global observational properties of the critical earthquake model, *Bull. Seismol. Soc. Am.* **9**, 1841–1855.

Papazachos, C.B., Karakaisis, G.F., Scordilis, E.M. and Papazachos, B.C., 2005b, New observational information on the precursory accelerating and decelerating strain energy release, *Tectonophysics*, (in press).

Robinson, R., 2000, A test of the precursory accelerating moment release model on some recent New Zealand earthquakes, *Geophys. J. Int.* **140**, 568–576.

Rosendahl, J.M., Vekic, M. and Rutledge, K.E., 1994, Probability of large avalanches on sand pile, *Phys. Rev. Lett.* **73**, 537–540.

Rundle, J.B., Klein, W. and Gross, S., 1996. Dynamics of a traveling density wave model for earthquakes, *Phys. Rev. lett.* **76**, 4285–4288.

Rundle, J.B., Klein, W., Turcotte, D.L. and Malamud, B.D., 2000, Precursory seismic activation and critical point phenomena, *Pure Appl. Geophys.* **157**, 2165–2182.

Sammis, C.G. and Smith, S.N., 1999, Seismic cycles and the evolution of stress correlation in cellular automation models of finite fault networks, *Pure Appl. Geophys.* **155**, 307–334.

Scholz, Ch.H., 1988, Mechanism of seismic quiescences, *Pure Appl. Geophys.* **26**, 701–718.

Scordilis, E.M., 2006, Empirical global relations converting M_S and m_b to moment magnitude, *J. Seismology*, (in press).

Scordilis, E.M., Papazachos, C.B., Karakaisis, G.F. and Karakostas, V.G., 2004, Accelerating seismic crustal deformation before strong mainshocks in Adriatic and its importance for earthquake prediction, *J. Seismology* **8**, 57–70.

Sornette, A. and Sornette, D., 1990, Earthquake rupture as a critical point. Consequences for telluric precursors, *Tectonophysics*, **179**, 327–334.

Sornette, D. and Sammis, C.G., 1995, Complex critical exponents from renormalization group theory of earthquakes: implications for earthquake predictions, *J. Phys. I.* **5**, 607–619.

Sykes, L.R. and Jaumé, S., 1990, Seismic activity on neighboring faults as a long term precursor to large earthquakes in the San Francisco Bay area, *Nature*, **348**, 595–599.

Tocher, D., 1959, Seismic history of the San Francisco bay region, *Calif. Div. Mines Spec. Rep.* **57**, 39–48.

Tzanis, A., Vallianatos, F. and Makropoulos, K., 2000, Seismic and electrical precursors to the 17-1-1983, M7 Kefallinia earthquake, Greece, signatures of a SOC system, *Phys. Chem. Earth (A)* **25**, 281–287.

Tzanis, A. and Vallianatos, F., 2003, Distributed power low seismicity changes and crustal deformation in the SW Hellenic arc, *Nat. Haz. Earth Sys. Sci.* **3**, 179–195.

Vanneste, C., and Sornette, D., 1992, Dynamics of rupture in thermal fuse models, *J. Phys. I.* **2**, 1621–1644.

Weatherley, D., Jaumé, S.C. and Mora, P., 2000. Evolution of stress deficit and changing rates of seismicity in cellular automation models of earthquake faults, *Pure Appl. Geophys.* **157**, 2183–2207.

Wessel, P. and Smith, W., 1995, New version of the Generic Mapping Tools, *EOS*, 76–329.

Wyss, M., 1997, Cannot earthquakes be predicted?, *Science*, **278**, 487–488.

Wyss, M., Klein, F. and Johnston, A.C., 1981, Precursors of the Kalapana M = 7.2 earthquake, *J. Geophys. Res.* **86**, 3881–3900.

Wyss, M. and Habermann, R.E., 1988, Precursory seismic quiescence, *Pure Appl. Geophys.* **126**, 319–332.

Zöller, G. and Hainzl, S., 2002, A systematic spatiotemporal test of the critical point hypothesis for large earthquakes, *Geophys. Res. Lett.* **29**, 53–57.

Zöller, G., Hainzl, S., Kurths, J. and Zschau, J., 2002, A systematic test on precursory seismic quiescence in Armenia, *Natural Hazards*, **26**, 245–263.